Two-photon transitions in confined hydrogenic atoms

Shalini Lumb[a], Sonia Lumb[b,*] and Vinod Prasad[c]
[a]*Department of Physics, Maitreyi College, University of Delhi, Delhi-110021, India*
[b]*Department of Physics and Electronics, Rajdhani College, University of Delhi, Delhi-110015, India.*
[*]*e-mail: sonia_lumb@hotmail.com*
[c]*Department of Physics, Swami Shraddhanand College, University of Delhi, Delhi-110036, India.*

Received 5 September 2017; accepted 27 October 2017

Two-photon transitions from ground state to excited and ionized states are studied. The energy levels and radial matrix elements of an impenetrable spherically confined hydrogenic atom embedded in plasma environment are evaluated using accurate Bernstein-polynomial (B-polynomial) method. Transition probability amplitudes, transparency frequencies and resonance enhancement frequencies for various transitions, namely, $1s-2s$, $1s-3s$ and $1s-3d$ are evaluated for various values of confining Debye potential parameter. The effect of spherical confinement is studied and explained.

Keywords: Two-photon transitions; confinement; Debye plasma; B-polynomials.

PACS: 32.30.-r; 32.70.-n; 32.80.-t

1. Introduction

Atomic and molecular systems confined in various plasma environments have occupied an important place in theoretical and experimental research fields [1–8]. It is well-known that in interpretation of various data associated with astrophysics, hot plasma etc., basic understanding of atomic excitation and ionization is required since these processes taking place in plasma environment provide important information about plasma. The processes which have recently attracted much attention are laser-assisted collisions in plasma [9–12] and response of confined atoms to short and intense laser pulses [13, 14]. The plasma environment considered here is Debye plasma where Debye screening length, $\lambda_D = \sqrt{k_B T/(4\pi e^2 n)}$, being a function of the plasma temperature T and its density n, plays an important role. Various sets of plasma conditions involved in real plasma environments can be simulated for one value of λ_D as one can evaluate the plasma temperature for a particular number density and vice-versa by fixing λ_D [15].

The screening of interaction potential between the nucleus and the electrons moving in atomic orbitals plays an important role in a variety of processes. In case of atoms and molecules confined under various conditions, the potential is modelled by a so-called Debye-Hückel potential [16]. The other form of screened potential called the exponential cosine screened coulomb potential, has long been used to describe an ionized impurity inside a semiconductor heterostructure [13, 15, 17, 18]. These screened potentials are prototype for many physical processes such as atoms confined in Debye or Debye-cosine plasmas, where atomic properties change drastically compared to free atoms, depending on the screening parameter, in particular [13, 15, 19–21]. The spectrum of the atom becomes quite interesting as reflected in its response to external fields. If, in addition to the screening potentials, there happens to be a spherical confinement, then the atom shows a drastic change in the spectrum. For example, Lumb *et al*. [14, 21] have shown that there are very few bound states if confining radius r_c is very small ($r_c \ll 10$ a.u.). So, spherical confinement in addition to screened potential forms a new confining potential where atomic and molecular systems are yet to be explored in detail. Impurities present in quantum dots are an example of a confined system where the spherical boundary represents the cage radius. In such practical physical situations the existing potential is modified due to interaction with impurities. As reported earlier [18], there have been few studies on the scattering processes taking place in confined environment. Two-photon spectroscopy has been an important tool to study the excitation of atoms and molecules ([22] and references therein). Two photon and three photon transitions in confined atoms under various kinds of confinements started receiving much attention since starting of 2000 [17, 23–29] as tools to study such transitions became available.

In the present study, we focus on the two-photon transitions in atomic hydrogen embedded in spherically confined Debye plasma. The model employed in the present case includes the effect of spatial confinement as well as screened Coulomb potential. The hydrogen atom is assumed to be embedded in plasma environment consisting of a finite charge distribution. The boundary condition signifies the finite extent of the charge cloud.The Debye confinement considered here is more likely to occur in many practical situations. In general, plasma environment in space is represented by this potential as is known from available literature. Also, the artificially created short-lived laboratory plasmas always have a finite volume. Such environments simulate the plasma present in interstellar space. Using the present model of confined plasma, simple Debye plasma model can be studied by enlarging the radius of confining sphere to infinity. Understanding of hydrogen atom under such confinement is important as it helps in examining more complex systems. Here, we consider electron of confined hydrogen atom being excited to

higher states through absorption of two photons. We study excitation from $1s$ to higher states. The effect of confinement on two-photon processes has been dealt with in detail. The spectrum of confined atom is evaluated using B-polynomial method [30–33].

The paper is organized according to the following scheme. The relevant theoretical details are provided in Sec. 2. The results of the present work are discussed in Sec. 3. Finally the important findings are summarized in Sec. 4.

2. Theory

The model considered here comprises a hydrogen atom embedded in a Debye plasma environment. The atom is assumed to be at the center of an impenetrable spherical cavity of radius r_0. This geometrically symmetric arrangement is a special case of the more general possibility in which the atom may be present at any position within the cavity. For simplicity, we have chosen the special case. Our aim here is to study the effect of spherical confinement and surrounding plasma on the two-photon transition probability amplitudes D_2, transparency frequency ω_t and resonance enhancement frequencies ω_r. This in turn requires a knowledge of the energy spectrum and the dipole matrix elements of the system. The spectrum, oscillator strengths and other physical quantities of confined systems are known to be highly dependent on the chosen confinement parameters and hence need an accurate evaluation. The evaluation of energy spectra and oscillator strengths of confined hydrogen in Debye plasma environment has been carried out and the results for various confining radii and Debye lengths characterizing different plasma conditions have been reported in our earlier works [15, 21]. The steps necessary for arriving at these results are summarized below for ready reference. We have used atomic units throughout our study.

The radial Schrödinger equation for the electron of the confined hydrogen atom is given by

$$\left[-\frac{1}{2}\frac{d^2}{dr^2} + \frac{l(l+1)}{2r^2} - \frac{1}{r}e^{-r/\lambda_D} + V_c(r) \right] U_{nl}(r) = E_{nl} U_{nl}(r) \qquad (1)$$

where $-e^{-r/\lambda_D}/r$ is the Debye-Hückel potential, $1/\lambda_D$ being the Debye screening parameter [34] and $V_c(r)$ is the confinement potential defined as

$$V_c(r) = \begin{cases} 0\,, & r < r_0 \\ \infty\,, & r \geq r_0. \end{cases}$$

The radial wave function $R_{n,l}(r) = U_{n,l}(r)/r$. $U_{n,l}(r)$ is expanded in B-polynomial basis as

$$U_{nl}(r) = \sum_{i=0}^{n} c_i B_{i,n}(r), \qquad (2)$$

where c_is are coefficients of expansion and $B_{i,n}(r)$ are B-polynomials of degree n. The confinement potential being infinite at the boundary, *i.e.*, $r = r_0$, forces the wave functions to vanish there. Under these restrictions the radial Schrödinger equation can be recast as a symmetric generalized eigenvalue equation in matrix form, given by

$$(A + F + G)C = EDC, \qquad (3)$$

where matrix elements $a_{i,j}, f_{i,j}, g_{i,j}$ and $d_{i,j}$ are defined as

$$a_{i,j} = \frac{1}{2}(B'_{i,n}, B'_{j,n}), \quad f_{i,j} = \frac{l(l+1)}{2}\left(\frac{B_{i,n}}{r^2}, B_{j,n}\right),$$
$$g_{i,j} = -\left(\frac{B_{i,n}}{r}e^{-r/\lambda_D}, B_{j,n}\right), \quad d_{i,j} = (B_{i,n}, B_{j,n}). \qquad (4)$$

The eigenvalues E provide the energy spectrum and eigenvectors C are used to calculate the corresponding radial wave functions using Eq. (3). We have used Fortran EISPACK library to solve Eq. (4).

The two-photon transition probability amplitude, D_2, of a hydrogen atom from the initial state $1s$ to a final state js can be evaluated by using [17, 24]

$$D_2 = \frac{1}{2}\sum_n \left[\frac{1}{-E_{1s} + E_n - \omega_0} + \frac{1}{-E_{js} + E_n + \omega_0} \right] \chi_1^n \chi_j^n \qquad (5)$$

where n represents the intermediate states including continuum, E_{1s} and E_{js} are the energy eigenvalues of the $1s$ and js states respectively and χ_1^n and χ_j^n are the dipole matrix elements defined as follows

$$\chi_k^n = \int_0^\infty r^3 R_n R_k dr, \qquad (k = 1, j) \qquad (6)$$

where R_l (with $l = n, k$) represents the radial wave function. The corresponding formula for calculating the transition probability amplitude for $1s$ to jd state is given by

$$D_2 = \frac{1}{\sqrt{5}}\sum_n \left[\frac{1}{-E_{1s} + E_n - \omega_0} + \frac{1}{-E_{jd} + E_n + \omega_0} \right] \chi_1^n \chi_j^n \qquad (7)$$

The values of ω_0 for which D_2 approaches infinity, and also lie inside the interval $\Delta E_{if}/2$ and ΔE_{if} are called the resonance enhancement frequencies, where ΔE_{if} is the difference between final and initial ($1s$) state energies [17]. Also, the frequencies for which the transition amplitude vanishes are called as the two-photon transparency frequencies [17].

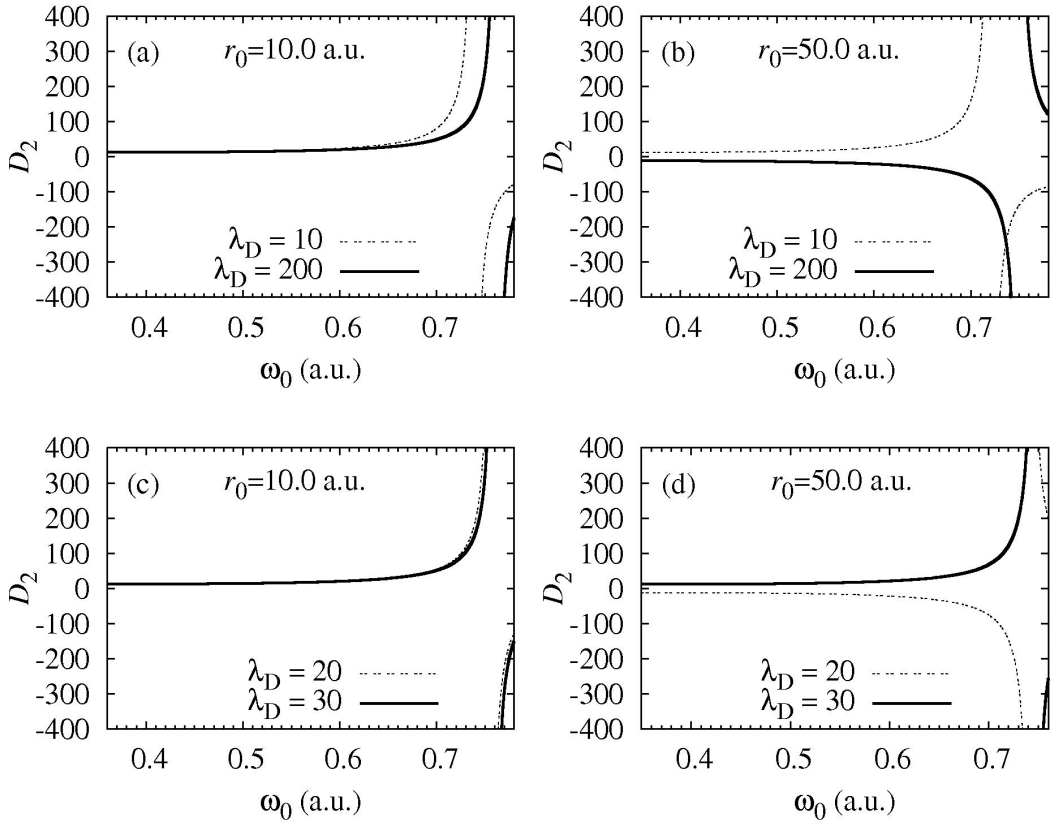

FIGURE 1. Variation of two-photon $1s-2s$ transition amplitude with frequency of incoming photons, ω_0, for various values of screening length λ_D.

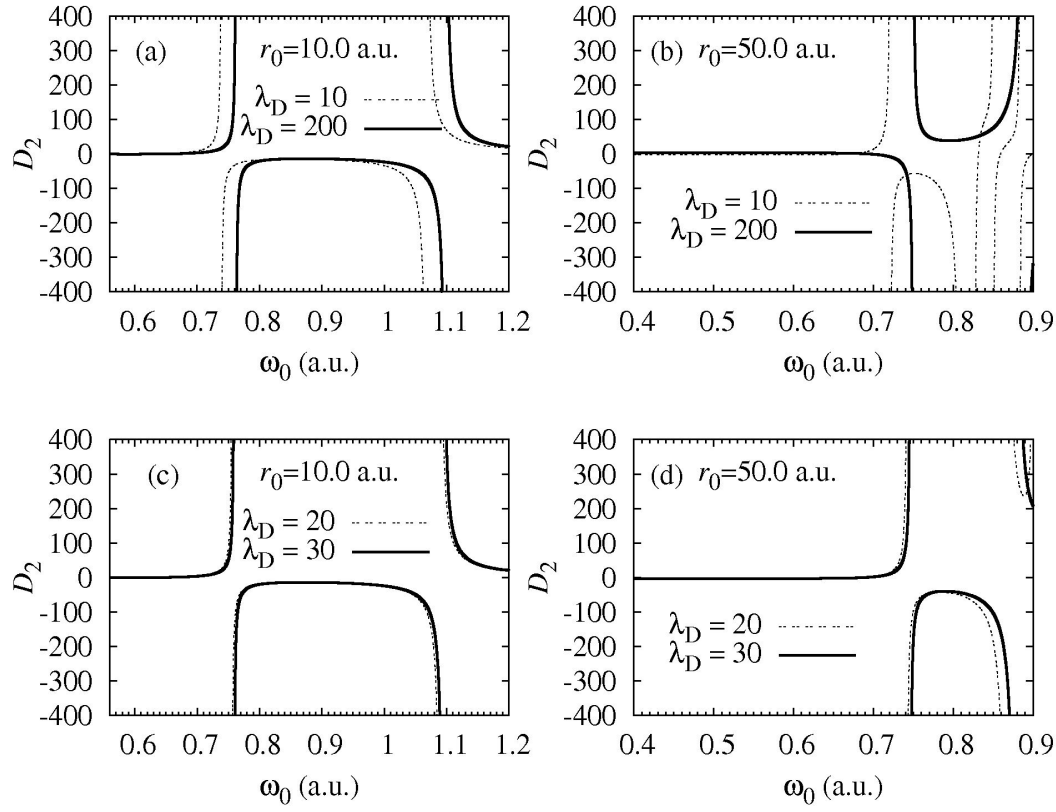

FIGURE 2. Same as Fig. 1 for $1s-3s$ transition.

3. Results and Discussions

The two-photon transition probability amplitudes of a hydrogen atom placed at the center of an impenetrable confining sphere of radius r_0 and embedded in a weak plasma characterized by Debye-Hückel potential are explored. Since Debye screening length λ_D is dependent on temperature and density of plasma, its different values represent different conditions of the system. We have explored the dependence of two-photon transitions on the extent of Debye screening as well as confinement radius. The probability amplitudes from $1s$ to js ($j = 2, 3, 4$) states have been calculated using Eq. (5) and to jd ($j = 3, 4$) states using Eq. (7) for a range of incident photon frequencies. It may be mentioned that the Hamiltonian being discretized leads to discreet continuum states, hence the quantum nature of the system is retained even for small confinements. Therefore, irrespective of the states being free or bound, the nomenclature of states is assumed to be same. The range of frequencies selected for studying the variation of two-photon transition probability amplitudes, transparency frequencies and resonance enhancement frequencies for various values of confinement parameters r_0 and λ_D is $\Delta E_{if}/2$ to ΔE_{if} as mentioned in Sec. 2.

The two-photon transition amplitudes as calculated by us show very close agreement with the previously available results in literature. For example, for a free hydrogen atom, the contributions to the $1s - 2s$ transition amplitudes due to first few intermediate states taking $\omega_0 = 0.375$ Ryd., given by Bassani *et al.* [35] match well with our results calculated for $r_0 = 50$ a.u. and $\lambda_D = \infty$. It may be noted that the spherical confinement radius $r_0 = 50$ a.u. is very large as compared to the size of hydrogen atom and hence corresponds to a nearly free atom. The total contribution calculated by them is -11.7805 and the value obtained in the present work is -11.7803. The energy levels, two-photon transition amplitudes, absorption coefficients, two-photon transparency frequencies and resonance enhancement frequencies as calculated by Paul and Ho [24] for a Debye plasma screened hydrogen atom are in consonance with our results for various values of λ_D. For example, the value of two-photon absorption coefficient for $1s - 2s$ transition based on our calculations is 144.8617 for $\lambda_D = 10$ a.u. and 138.8400 for $\lambda_D = 200$ a.u. taking $\omega_0 = 0.37$ Ryd. This data matches exactly with the results of Paul and Ho [24]. This provides a check on our calculations. The aim of the present work is to analyze the effect of spherical confinement on such properties of the system.

Figures 1-3 show variation of the two-photon transition probability amplitudes for four different values of λ_D, viz., 10, 20, 30 and 200 a.u. and two values of r_0, viz., 10 a.u. and 50 a.u. It is found that the two-photon transition probability amplitudes D_2 depend on both Debye and spherical confinement. Figure 1 which shows D_2 elements for $1s - 2s$ transitions clearly depicts the effect of change in Debye as well as spherical confinement. In Figs. 1(a) and (b), it is seen that if λ_D is varied over a wide range from 10 to 200 a.u., the resonance enhancement condition is achieved for small frequencies for smaller λ_D. Such variation is not much prominent for small change in λ_D as in Figs. 1(c) and (d). It is also evident from Fig. 1 that the nature of variation of D_2 changes with r_0. The resonance enhancement frequency shifts towards lower ω_0 for weaker spherical confinement. The variation with r_0 and λ_D as observed in Fig. 1 is also present in the data plotted in Figs. 2 and 3. These features can be explained on the basis of the change in energy spectrum and radial matrix elements with Debye as well as spherical confinement. The detailed structure of energy spectrum for such a confined system has been described in our earlier works [15, 21]. The decrease in number of bound states and increasing separation of the energy levels for smaller r_0 values are responsible for the observed behaviour. Figure 4 shows similar variation of D_2 for $r_0 = 15, 20$ and 40 a.u. and $\lambda_D = \infty$ for $1s - 2s$, $1s - 3s$, $1s - 3d$ and $1s - 4d$ transitions. It clearly depicts the effect of spherical confinement in absence of Debye screening.

The explicit values of transparency and resonance enhancement frequencies of two photon transition probability amplitudes are presented in Tables I-III. The frequencies corresponding to the transitions to $4s$ and $4d$ have also been included in the tables. The values for transitions to $2s$, $3s$ and $3d$ are also implicit in the graphical representation of two photon transition probability amplitudes shown in Figs. 1-4. The transparency frequency [17, 24] as observed for transitions to $3s$, $4s$ and $4d$ states have been reported in Table I. The plasma screening has been found to considerably affect the transparency frequencies. With decrease in λ_D for a fixed r_0, the transparency frequency, ω_t, also decreases as observed by Paul and Ho [24]. Similar effect has been observed for variation with confinement radius. That is, decrease in r_0 or increase in confinement leads to decrease in ω_t as shown in Table I. For the case of tight confinement, $r_0 = 10$ a.u., only a single transparency condition is obtained for $1s$ to $4s$ transition for all λ_D as compared to two transparency frequencies for rest of the r_0 values. This is due to the fact that transparency frequency is limited only to the range $\Delta E_{if}/2$ and ΔE_{if}.

The resonance enhancement frequencies obtained for transitions to $2s$, $3s$,$4s$, $3d$ and $4d$ levels are given in Tables II and III. These are found to be same for particular confinement radius and Debye length irrespective of the final state. The values for $1s - 3s$ transitions as calculated in the present work match very well with those quoted by Paul and Ho [24]. More frequencies correspond to resonance enhancement condition for transitions from $1s$ to $3s$ or $4s$ states on increasing the spherical confinement for some λ_D as can be seen from the data in Table III for $r_0 = 30$ and 50 a.u. An opposite trend is observed in the transitions from $1s$ to $3d$ or $4d$ states. The trend shows that confinement effect on probability of two-photon transition to a state depends on the shape of its orbital.

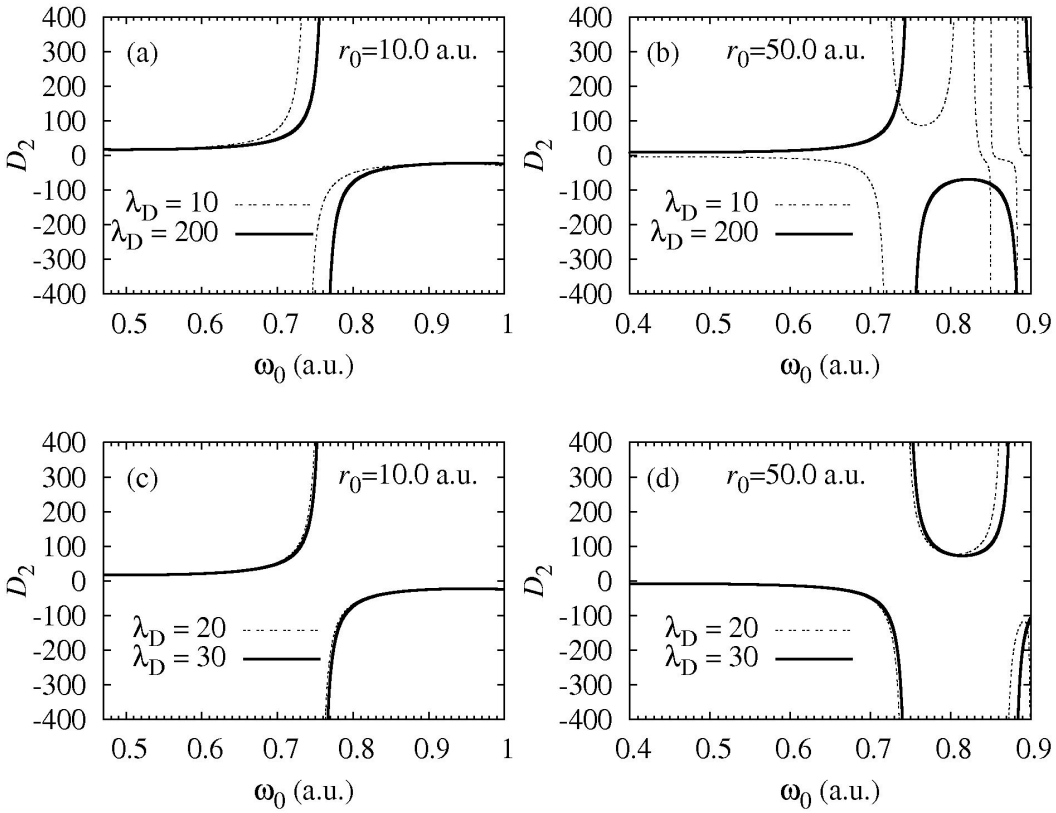

FIGURE 3. Same as Fig. 1 for $1s-3d$ transition.

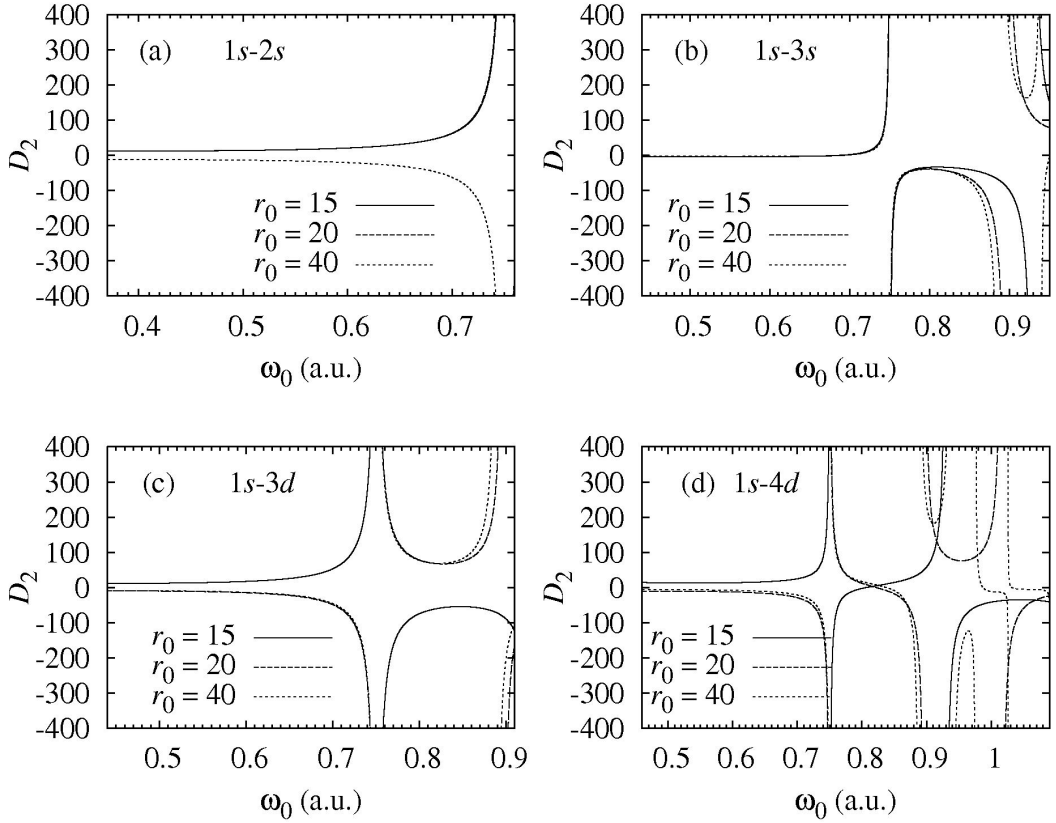

FIGURE 4. Variation of two-photon transition amplitudes for $1s-2s$, $1s-3s$, $1s-3d$ and $1s-4d$ transitions with frequency of incoming photons, ω_0, for screening length $\lambda_D = \infty$.

TABLE I. Two-photon transparency frequencies for various Debye screening lengths, λ_D, and confinement radii, r_0. The data is in atomic units. The results for $r_0 = 50$ a.u. have been compared with those of free hydrogen.

r_0	λ_D	$1s \to 3s$	$1s \to 4s$	$1s \to 4d$
10	10	0.6220155	1.0418125	0.7633365
	15	0.6374085	1.0439695	0.7783205
	20	0.6429075	1.0448025	0.7839785
	30	0.6469285	1.0454365	0.7882275
	200	0.6501865	1.0459845	0.7917615
15	10	0.6625705	0.6671255	0.7666505
			0.8144075	
	15	0.6761735	0.6771675	0.7875435
			0.8422595	
	20	0.6811455	0.6808125	0.7954565
			0.8532235	
	30	0.6848055	0.6834675	0.8014125
			0.8616995	
	200	0.6877845	0.6855815	0.8063935
			0.8690165	
20	10	0.6690395	0.6668105	0.7769765
			0.8026365	
	15	0.6819135	0.6787535	0.8011405
			0.8345025	
	20	0.6865375	0.6831165	0.8100715
			0.8471905	
	30	0.6899045	0.6863195	0.8166685
			0.8570665	
	200	0.6926055	0.6889105	0.8220685
			0.8656685	
30	10	0.6714915	0.6684855	0.7913775
			0.8003005	
	15	0.6835095	0.6806875	0.8172785
			0.8361105	
	20	0.6878315	0.6850525	0.8256905
			0.8501085	
	30	0.6909785	0.6882145	0.8313625
			0.8608235	
	200	0.6934965	0.6907285	0.8355395
			0.8699895	
50	10	0.6718395	0.6704785	0.8040815
		0.672[a]	0.8023525	
	15	0.6836195	0.6819315	0.8263675
		0.6835[a]	0.8385935	
	20	0.6878945	0.6859735	0.8318885
		0.688[a]	0.8521725	
	30	0.6910215	0.6888935	0.8354605
			0.8624345	
	200	0.6935135	0.6911895	0.8380465
		0.6935[*,a]	0.8711365	

[a] Reference [24].

[*] Value is for $\lambda_D = \infty$

TABLE II. Two-photon resonance enhancement frequencies for various Debye screening lengths, λ_D, and confinement radii, $r_0 = 10, 15$ and 20 a.u. The data is in atomic units.

r_0	λ_D	$1s \rightarrow 2s$	$1s \rightarrow 3s$	$1s \rightarrow 4s$	$1s \rightarrow 3d$	$1s \rightarrow 4d$
10	10	0.738714	0.738714	1.041836	0.738714	0.738714
			1.067930	1.067930		1.067930
				1.602878		
	15	0.751158	0.751158	1.044687	0.751158	0.751158
			1.083600	1.083600		1.083600
				1.617914		
	20	0.755824	0.755824	1.045969	0.755824	0.755824
			1.089686	1.089686		1.089686
				1.623756		
	30	0.759316	0.759316	1.047029	0.759316	0.759316
			1.094338	1.094338		1.094338
				1.628224		
	200	0.762209	0.762209	1.048002	0.762209	0.762209
			1.098282	1.098282		1.098282
				1.632017		
15	10		0.722295	0.722295	0.722295	0.722295
			0.881457	0.881457		0.881457
				1.107375		
	15		0.737215	0.737215	0.737215	0.737215
			0.905802	0.905802		0.905802
				1.130544		
	20		0.742775	0.742775	0.742775	0.742775
			0.915543	0.915543		0.915543
				1.139876		
	30		0.746927	0.746927	0.746927	0.746927
			0.923137	0.923137		0.923137
				1.147195		
	200	0.750373	0.750373	0.750373	0.750373	0.750373
			0.929743	0.929743		0.929743
				1.153608		
20	10		0.721122	0.721122	0.721122	0.721122
			0.834974	0.834974		0.834974
				0.954652		
	15		0.736483	0.736483	0.736483	0.736483
			0.865737	0.865737		0.865737
				0.984498		
	20		0.742172	0.742172	0.742172	0.742172
			0.878180	0.878180		0.878180
				0.996924		
	30		0.746412	0.746412	0.746412	0.746412
			0.887954	0.887954		0.887954
				1.006907		
	200		0.749925	0.749925	0.749925	0.749925
			0.896554	0.896554		0.896554
				1.015934		

TABLE III. Two-photon resonance enhancement frequencies for various Debye screening lengths, λ_D, and confinement radii, $r_0 = 30, 50$ a.u. The data is in atomic units. The results for $r_0 = 50$ a.u. have been compared with those of free hydrogen.

r_0	λ_D	$1s \to 3s$	$1s \to 4s$	$1s \to 3d$	$1s \to 4d$
30	10	0.721048	0.721048	0.721048	0.721048
			0.814992	0.814992	0.814992
			0.862225		
	15	0.736454	0.736454	0.736454	0.736454
			0.852222	0.852222	0.852222
			0.901888		
	20	0.742153	0.742153	0.742153	0.742153
			0.867094	0.867094	0.867094
			0.919349		
	30	0.746397	0.746397	0.746397	0.746397
			0.878668	0.878668	0.878668
			0.933938		
	200	0.749914	0.749914	0.749914	0.749914
		0.888793	0.888793		0.888793
			0.947785		
50	10	0.721044	0.721044	0.721044	0.721044
		0.721[a]	0.811171	0.811171	0.811171
					0.826633
	15	0.736459	0.736459	0.736459	0.736459
		0.736[a]	0.851124	0.851124	0.851124
					0.876753
	20	0.742160	0.742160	0.742160	0.742160
		0.742[a]	0.866526	0.866526	0.866526
					0.899727
	30	0.746409	0.746409	0.746409	0.746409
			0.878360	0.878360	0.878360
					0.918976
	200	0.749914	0.749914	0.749914	0.749914
		0.75[*,a]	0.888621	0.888621	0.888621
			0.937057		0.937057

[a] Reference [24].

[*] Value is for $\lambda_D = \infty$

4. Conclusions

The effect of spherical confinement on two-photon transition probability amplitudes, transparency frequencies and resonance enhancement frequencies for a Debye plasma embedded hydrogen atom has been explored. The spectrum of the atom has been calculated using B-polynomials. It is understood that experimental data for the confining potential undertaken in the present study is not available. However, the obtained results for loose spherical confinement ($r_0 = 50$ a.u.) have been compared with the theoretical results reported earlier in literature for some values of Debye parameter and no spherical boundary in Tables I and III. A close agreement has been achieved. It is anticipated that with the advancement of technology the present model of confining potential may become a reality in future and the data presented in the paper would be useful for such experimental studies. The spherical confinement is found to play a role analogous to Debye confinement. In particular, the transparency and resonance enhancement frequencies decrease with increase in confinement.

1. S. Ichimaru, *Rev. Mod. Phys.* **54** (1982) 1017.
2. N.C. Deb and N.C. Sil, *J. Phys. Murciélago Mol. Phys.* **17** (1984) 3587.
3. L.B. Zhao and Y.K. Ho, *Phys. Plasmas* **11** (2004) 1695.
4. J.S. Yoon and Y.-D. Jung, *Phys. Plasmas* **3** (1996) 3291.
5. *Electronic Structure of Quantum Confined Atoms and Molecules* (ed) K D Sen (Switzerland: Springer) (2014)
6. R. Kundliya, V. Prasad and M. Mohan, *J. Phys. B: At. Mol. Opt. Phys.* **33** (2000) 5263.
7. R. Khordad, *Indian J. Phys.* (2017) doi: 10.1007/s12648-017-0980-8
8. H. Hassanabadi, A.N. Ikot, C.P. Onyenegecha and S. Zarrinkamar, *Indian J. Phys.* (2017). doi: 10.1007/s12648-017-1009-z
9. W. Hong and Y.-D. Jung, *Phys. Plasmas* **3** (1996) 2457.
10. A.K Bhatia and C. Sinha, *Phys. Rev. A* **86** (2012) 053421.
11. M.K. Pandey, Y.-C. Lin and Y.K. Ho, *Phys. Plasmas* **22** (2015) 052104.
12. S. Mukhopadhyay and C. Sinha, *Phys. Rev. A* **88** (2013) 033414.
13. S. Lumb, S. Lumb and V. Prasad, *Phys. Rev. A* **90** (2014) 032505.
14. S. Lumb, S. Lumb and V. Prasad, *Indian J. Phys.* **89** (2015) 13.
15. S. Lumb, S. Lumb and V. Prasad, *Phys. Lett. A* **379** (2015) 1263.
16. S. Kar and Y.K. Ho, *Phys. Rev. A* **75** (2007) 062509.
17. S. Paul and Y.K. Ho, *Phys. Rev. A* **78** (2008) 042711.
18. S. Paul and Y.K. Ho, *Phys. Rev. A* **79** (2009) 032714.
19. M. Bassi and K.L. Baluja, *Indian J. Phys.* **86** (2012) 961.
20. S. Lumb, S. Lumb, D. Munjal and V. Prasad, *Phys. Scr.* **90** (2015) 095603.
21. S. Lumb, S. Lumb and V. Nautiyal, *Eur. Phys. J. D* **69** (2015) 176.
22. A. Quattropani, F. Bassani and S. Carillo, *Phys. Rev. A* **25** (1982) 3079.
23. H.F. Lai, Y.C. Lin and Y.K. Ho, *Journal of Physics: Conference Series* **163** (2009) 012096.
24. S. Paul and Y.K. Ho, *Phys. Plasmas* **15** (2008) 073301.
25. M.D. Lukin, *Rev. Mod. Phys.* **75** (2003) 457.
26. S. Paul and Y.K. Ho, *Phys. Plasmas* **16** (2009) 063302.
27. Y.K. Ho, H.F. Lai and Y.C. Lin, *Journal of Physics: Conference Series* **194** (2009) 022023.
28. S. Paul and Y.K. Ho, *Phys. Plasmas* **17** (2010) 082704.
29. A. Soylu, *Phys. Plasmas* **19** (2012) 072701.
30. M.I. Bhatti, *Adv. Studies Theor. Phys.* **3** (2009) 451.
31. M.I. Bhatti and W.F. Perger, *J. Phys. B: At., Mol. Opt. Phys.* **39** (2006) 553.
32. S. Lumb, S. Lumb and V. Prasad, *J. Mod. Phys.* **4** (2013) 1139.
33. S. Lumb, S. Lumb and V. Prasad, *Quantum Matter* **2** (2013) 314.
34. P. Debye and E. Hückel, *Z. Phys.* **24** (1923) 185.
35. F. Bassani, J.J. Forney and A. Quattropani, *Phys. Rev. Lett.* **39** (1977) 1070.